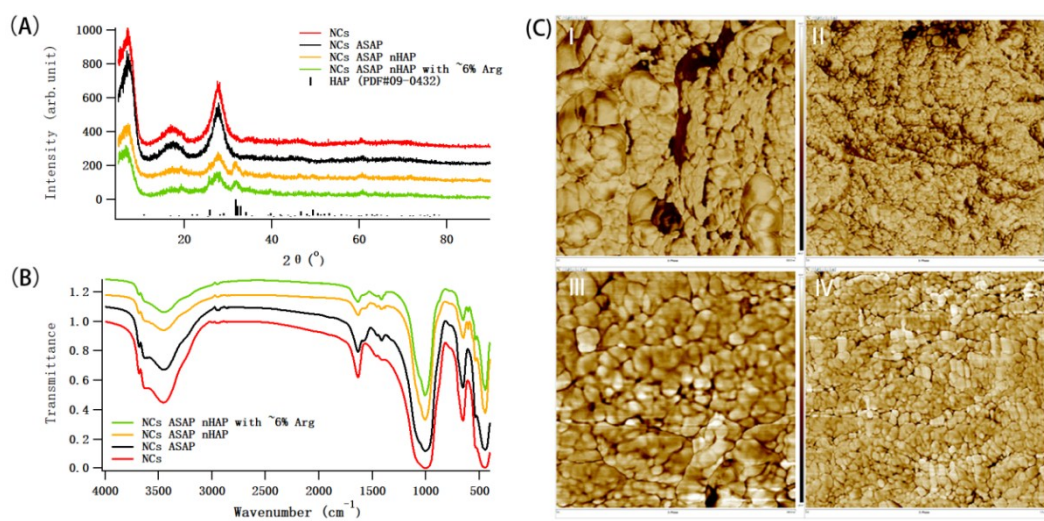
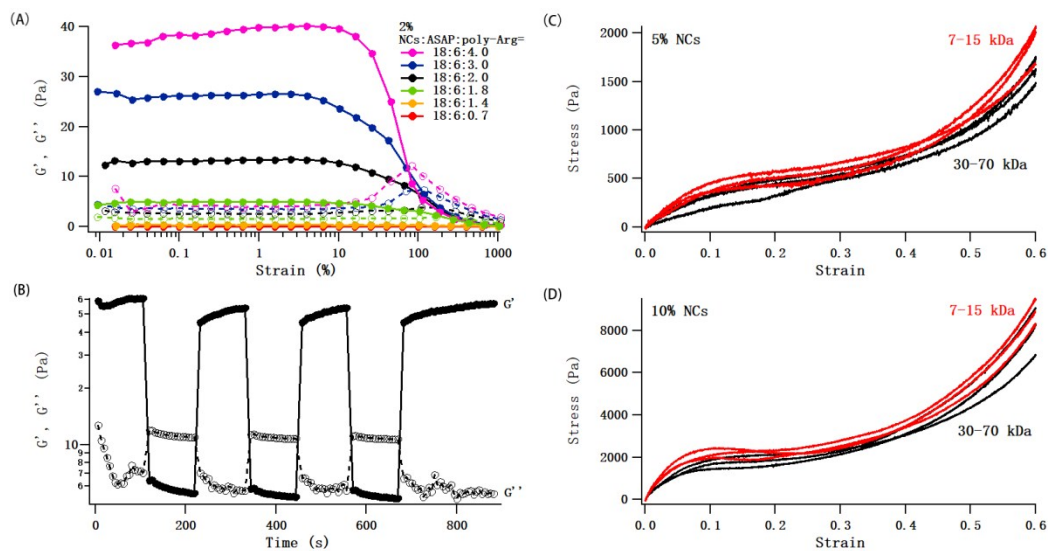


### Supplementary information



**Figure S1. Characterization of NC/nHAP composites.** A) XRD patterns and B) FTIR spectrum of the composites. C) AFM images of composites based on NCs with (I and II) nHAP and (III and IV) Arg-modified nHAP, respectively.



**Figure S2. Mechanical properties of the physically crosslinked gels based on nano-clays (NCs) and poly-Arg.** A) Rheological properties of 2% gels with different amounts of poly-Arg in strain-sweeping mode. B) Changes of storage moduli  $G'$  and loss modulus  $G''$  of the 2% gels with a charge ratio of  $[NCs (-)]:[poly-Arg (+)]:[ASAP (-)] = 18.0:4.0:6.0$  in continuous step strain measurements. Representative stress-strain curves obtained from compressive mechanical tests on the C) 5% and D) 10% gels. No significant influence of the molecular weight of poly-Arg was observed.

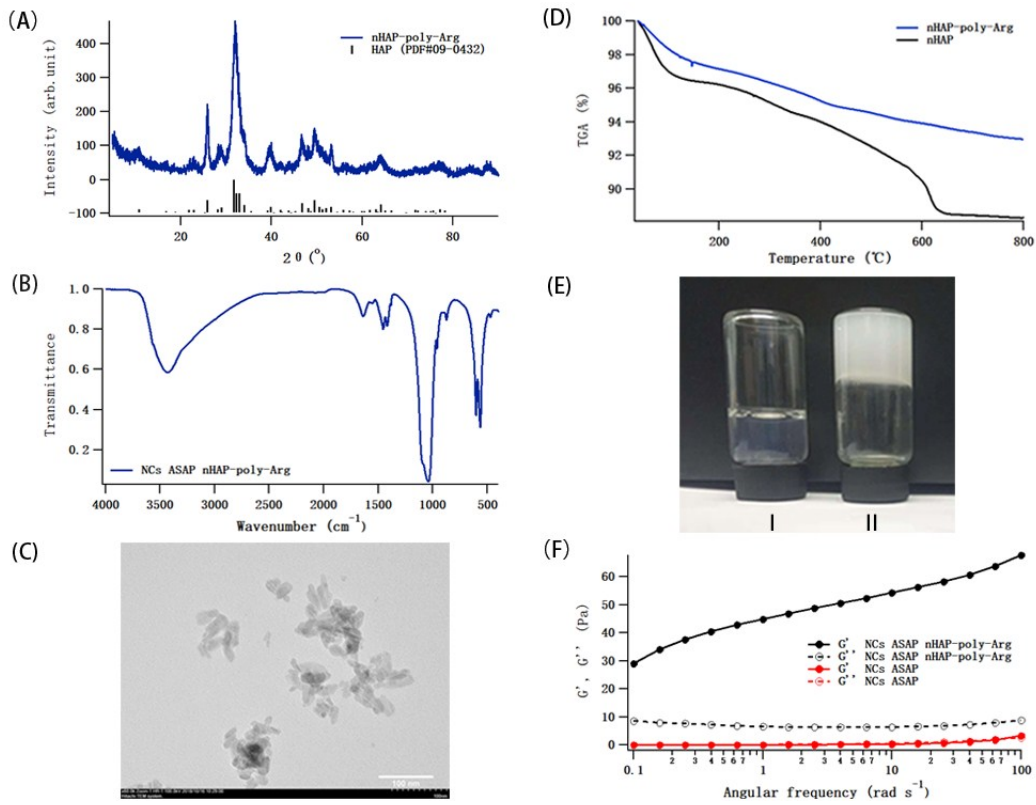


**Figure S3. Formation of physically crosslinked gels based on nano-clays (NCs) and nHAP-poly-Arg.** A) XRD patterns, B) FTIR spectrum and C) TEM images of nHAP-poly-Arg. D) TGA measurements of nHAP and nHAP-poly-Arg in the temperature range of [40, 800] $^{\circ}\text{C}$ . Coating efficiency of poly-Arg was calculated to be  $\sim 4.68\%$ . E) Photographs of 10% NCs (pre-treated with ASAP) without (left) and with (right) 30 mg nHAP-poly-Arg, corresponding to a charge ratio of  $[\text{NCs} (-)]:[\text{nHAP} - \text{poly} - \text{Arg} (+)]:[\text{ASAP} (-)] = 18.0:1.8:6.0$ . F) Rheological properties of the resultant gels in frequency-sweeping mode.

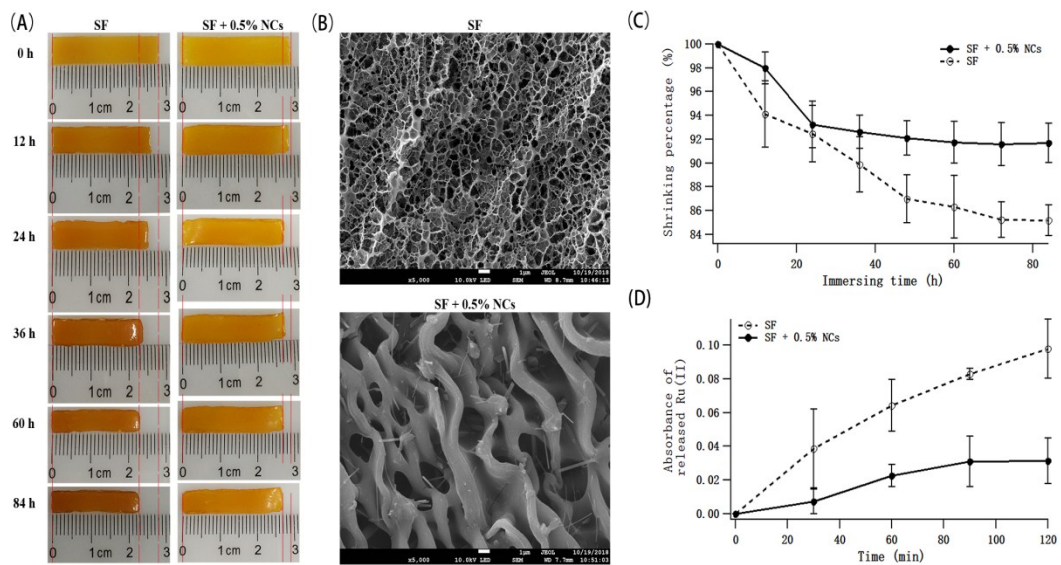


**Figure S4. Properties of chemically crosslinked SF-based hydrogels in the presence and absence of physically crosslinked NC-based network.** A) Photographs, B) SEM images, C) shrinking and D) Ru(II)-releasing profiles of the hydrogels after being immersed in deionized water for certain time periods.